# Structural investigation of La$_{9.33}$Si$_6$O$_{26}$- and La$_9$AESi$_6$O$_{26+\delta}$-doped apatites-type lanthanum silicate (AE = Ba, Sr and Ca) by neutron powder diffraction

S. Lambert[a],*, A. Vincent[a], E. Bruneton[a], S. Beaudet-Savignat[a], F. Guillet[a], B. Minot[a], F. Bouree[b]

[a]CEA Le Ripault, BP 16 37260 MONTS, France
[b]LLB CEA Saclay, 91191 GIF sur YVETTE, France

## Abstract

Crystalline structures of La$_{9.33}$Si$_6$O$_{26}$ and La$_9$AESi$_6$O$_{26+\delta}$ (AE = Ba, Sr and Ca) doped apatites-type lanthanum silicates were investigated by X-ray and neutron powder diffraction at room temperature. The results obtained after different models testing show that the apatite structure is best described using the $P6_3$ space group. The loss of the mirror symmetry perpendicular to the ionic conduction channel direction results from heterogeneous La$^{3+}$/AE$^{2+}$ distribution of the sites so-called "4$f$". The Rietveld refinements do not show splitting of the conduction oxygen $(0,0,\frac{1}{4})$ site but rather a very large spread of the nuclear density associated to this site. This effect is more pronounced for the La$_9$AESi$_6$O$_{26+\delta}$-doped compounds. Large anisotropic thermal displacement parameters are also observed for the oxygens associated to the isolated [SiO$_4$], suggesting a rotation of this tetrahedron around the Si site. Lastly, vacancies were also systematically observed in the lanthanum nine-coordinated sites.
© 2006 Elsevier Inc. All rights reserved.

Keywords: Apatite; Lanthanum silicate; X-ray diffraction; Neutron diffraction; Nuclear density spread

## 1. Introduction

A number of oxide ion conductors are being developed for an application as solid electrolytes in solid oxide fuel cells (SOFCs). Among them, lanthanum silicates with an apatite-type structure are of great interest as their conductivities are higher than for the yttria-stabilized zirconia (YSZ) electrolyte at intermediate temperature (600–800 °C) [1–5]. The apatite structure (Fig. 1) is built up from isolated [SiO$_4$]$^{3-}$ tetrahedrons with La$^{3+}$ cations located in 7 and 9 coordinated sites. The framework exhibits channels along the $c$-axis where oxide ions migrate [2,6,7]. The conduction oxygen is generally described by a single site with large anisotropic thermal displacement parameters (ADPs) [6,8–10] but a splitting of the $(0,0,\frac{1}{4})$

site [11] leading to a positional disorder inside the apatite structure is also reported [12].

The ionic conductivity of these materials [13] depends directly on the oxygen ratio inside the apatite-type compounds. High oxide ion conductivity values [5,11,14,15] were reported in the literature for the La$_{10-y}$M$_6$O$_{26+\delta}$ (M = Si or Ge) with $\delta > 0$. It is usually very difficult to directly quantify this ratio but considering respectively the $+3$, $+2$ and $+4$ valences for La, AE and Si ions in the structure, the $\delta$ value can be estimated from the electroneutrality of the compound. The conductivity shows anisotropic behaviour and the mechanism explaining the high conduction values is a subject of controversy in the literature through two main models. The first one proposes a relationship between structure and ionic conduction with a migration of the oxide ions along the [001] channels according to a linear path [13]. The second model proposed recently by Léon-Reina et al. [2] is based on the existence of extra oxygen sites in the apatite

*Corresponding author.
E-mail address: sebastien.lambert@cea.fr (S. Lambert).

structure and from a pseudo-sinusoidal path [11,13] with a complicated interstitial migration. These new sites, depending of the chemical composition and in particular of the $\delta$ value, were determined by neutron powder diffraction. The interstitial oxygen site is located at (0.013, 0.232, 0.616) or (−0.001, 0.224, 0.580) position [2,6] for $La_{9.33}Si_6O_{26}$ and $La_{9.55}Si_6O_{26.32}$, respectively, with oxygen vacancies at the centre of the channels $(0, 0, \frac{1}{4})$. It should be noted that in this study, this new site was weakly occupied by oxygen atoms (less than 2%). The lanthanum silica apatites also usually exhibit significant number of cationic vacancies on the 9-coordinated La(1) and La(2) sites [9–12] (Fig. 1).

An accurate structural description of the oxygens network is thus very important to understand of the relationship between the structure and oxygen ion transport in apatite-type electrolytes. The present paper reports the structural investigation by neutron powder diffraction of undoped $La_{9.33}Si_6O_{26}$ and doped $La_9AESi_6O_{26+\delta}$ ($AE$ = Ba, Sr and Ca) lanthanum silica apatites. Structural

adjustments are discussed in comparison with similar compounds.

## 2. Experimental section

Pure lanthanum silica apatites are very difficult to obtain with high purity because the samples could be often contaminated either with $La_2SiO_5$ or $La_2Si_2O_7$ secondary phases. The powders were prepared by standard high temperature solid-state reaction starting from a stoichiometric mixture of $La_2O_3$ (Rhodia 99.99%), $SiO_2$ (Cerac 99.99%) and $BaCO_3$ (Cerac 99.99%), $SrCO_3$ (Alfa Aesar, 99.99%) or $CaCO_3$ (Cerac 99.99%) precursors, according to the chemical formula $La_{9.33}Si_6O_{26}$, $La_9Ba_1Si_6O_{26+\delta}$, $La_9Sr_1Si_6O_{26+\delta}$, $La_9Ca_1Si_6O_{26+\delta}$, respectively. The preparation procedure of dense samples was described elsewhere [1,4].

Structural characterisations were first performed by X-ray powder diffraction at room temperature using a Bruker-Siemens D5000 diffractometer using copper radiation. No secondary crystalline phase was detected. The cell parameters (Table 1) were refined by the least-square method from diffraction patterns obtained with appropriate mixtures of the studied lanthanum silicate apatites with a position standard (NIST 640c Si). This procedure ensures an accurate measurement of the diffraction peak position. A broadening of the lines profiles is observed on the X-ray diffraction patterns in comparison with the instrumental function of the used diffractometer. This phenomenon is observed for all diffraction peaks and it is not pronounced for particular *hkl* direction. It cannot be attributed to a particle size effect because the grains exhibit a size of around few microns.

Neutron powder diffraction (NPD) experiments were performed at the Orphée reactor at Léon Brillouin Laboratory (CEA/Saclay France), on high-resolution 3T2 diffractometer using a Ge(335) monochromator and a wavelength $\lambda = 1.2251$ Å. The patterns were measured at room temperature in the range $6° < 2\theta < 120°$ in steps of
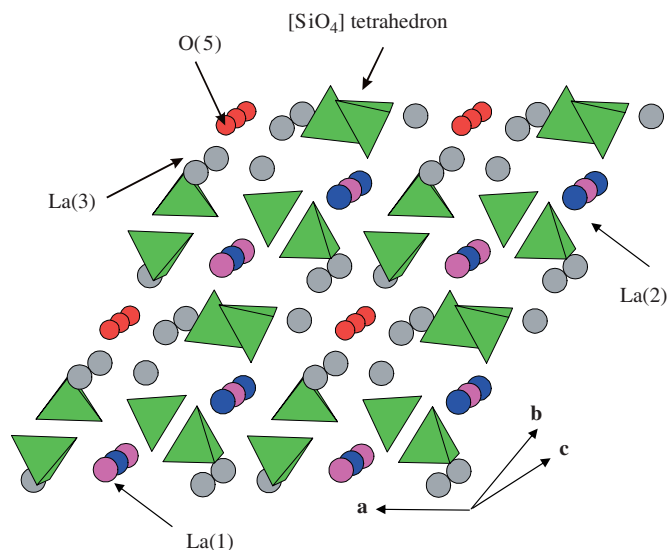


Fig. 1. Crystal structure of lanthanum silica apatite.

Table 1
Refinement parameters

| Compound | $La_{9.33}(SiO_4)_6O_2$ | $La_9Ba\ (SiO_4)_6O_{2+\delta}$ | $La_9Sr\ (SiO_4)_6O_{2+\delta}$ | $La_9Ca\ (SiO_4)_6O_{2+\delta}$ |
|---|---|---|---|---|
| $a$ (Å) XRD | 9.725(5) | 9.740(5) | 9.705(5) | 9.680(5) |
| $b$ (Å) XRD | 7.189(5) | 7.267(5) | 7.215(5) | 7.161(5) |
| $a$ (Å) NPD | 9.7284(2) | 9.7422(2) | 9.7058(2) | 9.6817(2) |
| $b$ (Å) NPD | 7.1868(2) | 7.2679(2) | 7.21302) | 7.1593(2) |
| $V$ (Å$^3$) | 589 | 597 | 588 | 581 |
| | | | | |
| Space group | $P6_3$ | | | |
| $\lambda$ (Å) | 1. 2251 | | | |
| Reliability factors (%) | | | | |
| $R_{obs}/R_{wobs}$ | 2.81/2.83 | 1.61/1.38 | 1.82/1.70 | 1.33/1.41 |
| $R_p/R_{Bragg}$ | 1.79/2.28 | 1.73/2.25 | 1.73/2.18 | 1.75/2.26 |
| Reflection number | 1253 | 1181 | 1170 | 1160 |
| Refined parameter number | 65 | 78 | 74 | 69 |
| Density residua (in comparison with nuclear density of one oxygen) | — | 5.5% | 4.2% | 4.2% |

0.05°. The neutron powder diffraction data were refined using the *JANA2000* program package [16]. The final refinement results are given in Tables 1–3.

## 3. Structural refinement

The apatite structure usually shows a hexagonal symmetry in the literature [4,6,9,11]. The cell parameters deduced from the apatite-Si position standard mixture X-ray diffraction patterns are identical to the values obtained from neutron powder diffraction within the limits of uncertainty. The variation of the cell volumes shows a linear increase with the cationic mean radius $r$ of the "4f" sites ($r = \sum_i q_i r_i$ where $r_i$ corresponds to the radius of the $i$ cationic element for a 9-coordinated site [17] and $q_i$ the ratio of these ions in the apatite structure (Table 2)). The apatite framework is expanded along all direction when the $Ca^{2+}$ is replaced by a $Ba^{2+}$ ion (Table 1). Indeed the cell parameters and the unit cell increase with the radius of the $AE$ atom for the studied chemical formula. Different possible space groups (SG) are usually tested in the structural investigations of the lanthanum silica apatites-type compounds. In accordance with these previous

studies, three SG were considered for the refinement of the neutron powder diffraction patterns: $P6_3/m$ (No. 176), $P6_3$ (No. 173) and $P$-3 (No. 143). The $B_{ij}$ or $U_{ij}$ ADPs [18] were used for all atomic positions. The refined structures were based on the apatite framework (Fig. 1). The best results (Figs. 2 and 3) were obtained using the $P6_3$ symmetry which led to the smaller reliability factors [16] $R_{obs}$ and $R_{wobs}$ values (Table 1). The main difference between the $P6_3/m$ and $P6_3$ SGs lies in the $m^{[001]}$ symmetry element, which exists only in the centro-symmetrical SG. The loss of this symmetry element requires us to consider two independent lanthanum sites, denoted La(1) and La(2) for (1/3, 2/3, z) and (2/3, 1/3, z') respectively, for the "4f" cationic positions. The Rietveld refinement shows in fact that these two sites exhibit some position correlations ($z \sim z'$) but their relative occupation is uncorrelated. Nonetheless, the framework exhibits a pseudo-symmetry "$P6_3/m$" because the symmetry breaking of the $m^{[001]}$ is very slight. The $P$-3 symmetry, proposed by Samson et al. [11,12] for the study of the $La_{9.33}Si_6O_{26}$ and $La_8Sr_2Si_6O_{26}$ compounds, became less evident ($R_{obs} > 3.5\%$) in comparison with the obtained results for the four studied samples (Table 1).

Table 2
Refined structural parameters from NPD data for non-doped and doped lanthanum silica apatites at room temperature

| Compounds | $La_{9.33}(SiO_4)_6O_2$ | $La_9Ba\,(SiO_4)_6O_{2+\delta}$ | $La_9Sr\,(SiO_4)_6O_{2+\delta}$ | $La_9Ca\,(SiO_4)_6O_{2+\delta}$ |
|---|---|---|---|---|
| La(1)/$AE$(1), (1/3, 2/3, z) | | | | |
| Occup. | 0.85(2) | 0.71(7)/0.29(7) | 0.45(1)/0.5[‡] | 0.64(6)/0.36(6) |
| z | −0.003(1) | 0.00(1) | 0.004(1) | 0.007(2) |
| La(2)/$AE$(2), (1/3, 2/3, z) | | | | |
| Occup. | 0.93(2) | 0.75(7)/0.25(7) | 1[‡]/ 0 | 0.73(6)/0.27(6) |
| z | −0.003(1) | 0.00(1) | 0.004(1) | 0.007(2) |
| La(3)/$AE$(3), (x, y, 1/4) | | | | |
| Occup. | 0.99(1) | 1 | 1 | 1 |
| x | 0.2310(2) | 0.2281(2) | 0.2276(1) | 0.2262(1) |
| y | −0.0132(2) | −0.0118(2) | −0.0121(1) | −0.0132(2) |
| Si (x, y, 1/4) | | | | |
| x | 0.4009(3) | 0.4015(1) | 0.4010(2) | 0.4030(3) |
| y | 0.3715(3) | 0.3720(2) | 0.3736(3) | 0.3736(3) |
| O(1) (x, y, 1/4) | | | | |
| x | 0.3216(3) | 0.3185(3) | 0.3218(2) | 0.3259(2) |
| y | 0.4825(4) | 0.4824(3) | 0.4832(2) | 0.4881(2) |
| O(2) (x, y, z) | | | | |
| x | 0.5940(2) | 0.5935(2) | 0.5953(2) | 0.5971(2) |
| y | 0.4726(3) | 0.4728(3) | 0.4729(2) | 0.4713(3) |
| z | 0.245(2) | 0.239(2) | 0.246(2) | 0.243(2) |
| O(3) (x, y, z) | | | | |
| x | 0.3293(10) | 0.333(5) | 0.333(7) | 0.333(5) |
| y | 0.2499(9) | 0.2508(7) | 0.2534(3) | 0.2529(6) |
| z | 0.416(2) | 0.419(1) | 0.426(1) | 0.430(2) |
| O(4) (x, y, z) | | | | |
| x | 0.3537(8) | 0.3524(5) | 0.3494(3) | 0.3546(4) |
| y | 0.2579(9) | 0.2599(9) | 0.2551(9) | 0.2620(7) |
| z | 0.058(2) | 0.062(1) | 0.067(1) | 0.0710(7) |
| O(5) (0, 0, 1/4) | | | | |

[‡] Fixed during the refinement.

Table 3
Refined anisotropic displacement parameters for non-doped and doped lanthanum silica apatites

| Compounds | $La_{9.33}(SiO_4)_6O_2$ | $La_9Ba\ (SiO_4)_6O_{2+\delta}$ | $La_9Sr\ (SiO_4)_6O_{2+\delta}$ | $La_9Ca\ (SiO_4)_6O_{2+\delta}$ |
|---|---|---|---|---|
| La(1), La(2) | | | | |
| $U_{11}$ | 0.0105(7) | 0.0102(7) | 0.0124(5) | 0.0134(7) |
| $U_{22}$ | 0.0105(7) | 0.0102(7) | 0.0124(5) | 0.0134(7) |
| $U_{33}$ | 0.031(2) | 0.014(1) | 0.0096(8) | 0.018(1) |
| $U_{12}$ | 0.005(4) | 0.0051(3) | 0.0062(2) | 0.0067(3) |
| $U_{23} = U_{13} = 0$ | | | | |
| La(3) | | | | |
| $U_{11}$ | 0.0106(7) | 0.0118(8) | 0.0111(6) | 0.0152(7) |
| $U_{22}$ | 0.0082(7) | 0.0077(7) | 0.0103(5) | 0.0104(7) |
| $U_{33}$ | 0.0103(7) | 0.0167(8) | 0.0094(4) | 0.0113(6) |
| $U_{12}$ | 0.0042(7) | 0.0054(7) | 0.0051(5) | 0.0043(6) |
| $U_{23}$ | 0 | 0.011(1) | 0 | -0.011(1) |
| $U_{13} = 0$ | | | | |
| Si | | | | |
| $U_{11}$ | 0.008(1) | 0.010(1) | 0.0084(8) | 0.005(1) |
| $U_{22}$ | 0.007(1) | 0.002(1) | 0.0044(8) | 0.006(1) |
| $U_{33}$ | 0.006(1) | 0.018(1) | 0.010(1) | 0.015(1) |
| $U_{12} = U_{23} = U_{13} = 0$ | | | | |
| O(1) | | | | |
| $U_{11}$ | 0.028(1) | 0.027(1) | 0.0110(7) | 0.024(1) |
| $U_{22}$ | 0.032(2) | 0.020(1) | 0.0064(6) | 0.013(1) |
| $U_{33}$ | 0.033(2) | 0.021(1) | 0.019(1) | 0.023(1) |
| $U_{12}$ | 0.026(1) | 0.019(1) | 0 | 0.014(1) |
| $U_{23}$ | 0.023(2) | -0.007(1) | 0 | 0 |
| $U_{13} = 0$ | | | | |
| O(2) | | | | |
| $U_{11}$ | 0.0116(9) | 0.0089(9) | 0.0074(6) | 0.012(1) |
| $U_{22}$ | 0.0077(8) | 0.0095(8) | 0.0085(6) | 0.009(1) |
| $U_{33}$ | 0.021(1) | 0.025(2) | 0.017(1) | 0.032(2) |
| $U_{12}$ | 0 | 0 | 0 | 0.0039(9) |
| $U_{23} = U_{13} = 0$ | | | | |
| O(3) | | | | |
| $U_{11}$ | 0.081(4) | 0.045(3) | 0.052(3) | 0.081(4) |
| $U_{22}$ | 0.005(2) | 0.006(2) | 0.007(2) | 0.002(2) |
| $U_{33}$ | 0.015(2) | 0.013(2) | 0.018(2) | 0.011(2) |
| $U_{12}$ | 0.015(2) | 0.008(2) | 0.013(2) | 0;011(2) |
| $U_{23}$ | 0.009(2) | 0.014(2) | 0.026(2) | 0.031(2) |
| $U_{13}$ | 0.033(2) | 0 | 0.012(2) | 0.017(1) |
| O(4) | | | | |
| $U_{11}$ | 0.030(2) | 0.026(2) | 0.032(2) | 0.041(2) |
| $U_{22}$ | 0.021(2) | 0.029(3) | 0.025(3) | 0.039(3) |
| $U_{33}$ | 0.012(2) | 0.011(2) | 0.008(2) | 0.028(3) |
| $U_{12}$ | 0.015(2) | 0.022(2) | 0.025(2) | 0.039(2) |
| $U_{23}$ | 0 | 0 | 0.003(1) | 0 |
| $U_{13}$ | 0 | 0 | 0.002(2) | 0 |
| O(5) | | | | |
| $U_{11}$ | 0.008(2) | 0.012(2) | 0.010(1) | 0.008(2) |
| $U_{22}$ | 0.008(2) | 0.012(2) | 0.010(1) | 0.008(2) |
| $U_{33}$ | 0.034(3) | 0.177(9) | 0.181(7) | 0.30(1) |
| $U_{12}$ | 0.0042(7) | 0.0064(8) | 0.0048(6) | 0.0040(9) |
| $U_{23} = U_{13} = 0$ | | | | |

During the NPD refinements of the *AE*-doped apatite samples, the La(3) density Fourier map (Fig. 4) could be only explained by a full occupation of this site by lanthanum atoms. As a consequence, the divalent cations would be preferentially positioned on the La(1) and/or La(2) sites. For the $La_9Sr_1Si_6O_{26+\delta}$ sample, the NPD structural refinement exhibits that the La(2) site nuclear density is better described only from lanthanum atoms.

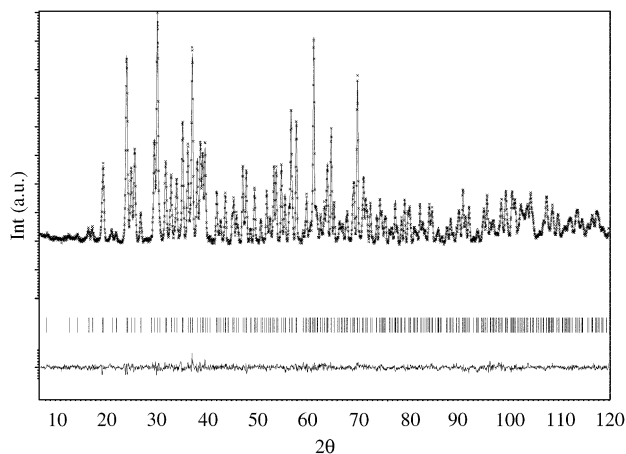Fig. 2. Observed (+), calculated (−) and difference powder neutron diffraction profiles for the non-doped apatite $La_{9.33}(SiO_4)_6O_2$.



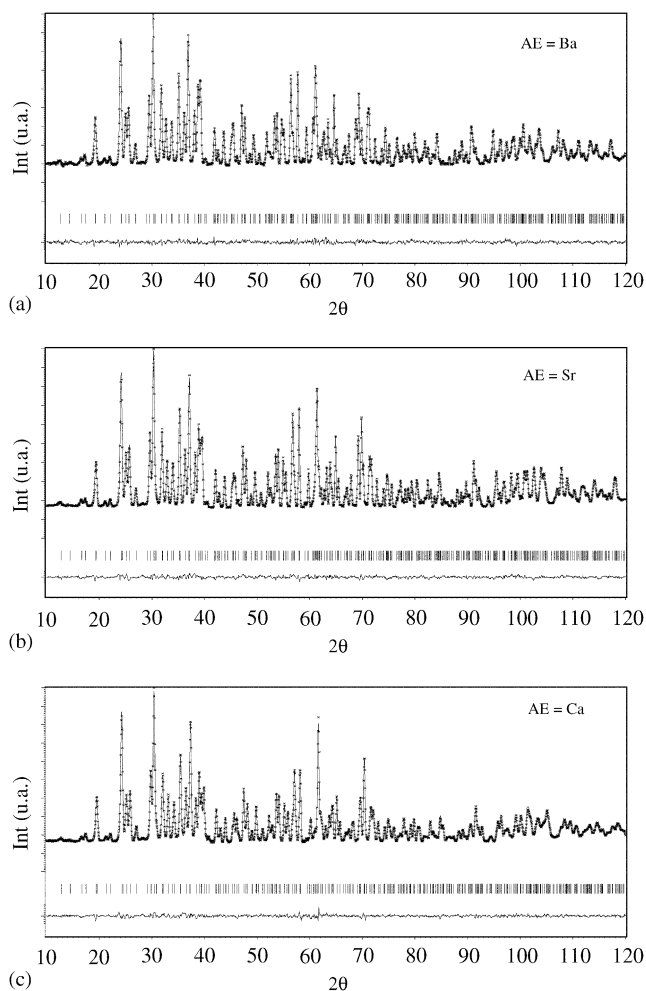Fig. 3. Observed (+), calculated (−) and difference powder neutron diffraction profiles for the doped apatite $La_9AE(SiO_4)_6O_{2+\delta}$, (a–c) for $AE$ = Ba, Sr and Ca, respectively.

From this result, it is possible to consider that the Sr atoms are located only on the La(1) site. Unfortunately, the nuclear density could not be correctly described when the

La(1) site is occupied randomly by La, Sr (occupation fixed from chemical formula) and (□) vacancies. A refinement of the La(1) site based from only La and Sr atoms leads to a Sr ratio superior to real chemical formula. Considering +3, +2, +4 and −2 valences for La, Sr, Si and O atoms, respectively, the sample electroneutrality is obtained with an extra oxygen ratio $\delta = 0.35$. The NPD refinement of the $La_9AESi_6O_{26+\delta}$ samples ($AE$ = Ba and Ca) shows that the La(2) site is not fully occupied by lanthanum atoms and that La, $AE$ and (□) vacancies should be randomly distributed on the La(1) and La(2) sites. Unfortunately, it was not possible to accurately determine the $AE/□$ ratios on each site during the NPD refinement procedure. The La(1) and La(2) sites were thus assumed to be only occupied by lanthanum and alkaline-earth atoms. The $AE$ ratios obtained for the last refinement are probably weakly overestimated.

## 4. Discussion

For the four studied samples, the final NPD refinements show that the best results are obtained using the $P6_3$ SG and the atomic framework corresponds to an apatite-type structure. No splitting of the conduction oxygen in the channels is observed in the structure. This position disorder was proposed by Samsom et al. [11] in the study of the $La_{9.33}Si_6O_{26}$ and $La_8Sr_2Si_6O_{26}$ compounds, although this study was performed using negative values for the $B_{ii}$ anisotropic thermal displacement parameters. A large spread of the conduction oxygens O(5) density is systematically observed in the Fourier maps (Fig. 4a and 5) along the c-axis direction leading to high $U_{33}$ ADPs values, which are obtained in the structural investigations of the apatite-type compounds [9,10,12]. The nuclear density maximum is located on the $(0, 0, \frac{1}{4})$ site and not above or below the pseudo-mirror plan. The structural model based from a split position of the conduction oxygen cannot obtain the better description of the O(5) site for the studied samples. These large ADPs could not be only attributed to thermal motion and show probably a static disorder from the ideal $(0, 0, \frac{1}{4})$ position [9]. A wide spread of the O(5) oxygen density is observed for the $AE$-doped compounds (Fig. 5, $AE$ = Ba). No oxygen atoms vacancy is observed in the conduction channels. Indeed, the introduction of vacancy in the structural refinement does not lead to an accurate description of the conduction oxygen nuclear density. It should be noted that the La(3) neighbouring sites are fully occupied by lanthanum atoms. The oxygens of the $[SiO_4]^{3-}$ tetrahedrons exhibit large ADPs in the (a, b) hexagonal plane in comparison with the $U_{33}$ values, as observed in the $Sr_2RE_8(SiO_4)_6O_2$ ($RE$ = La and Nd) compound [7]. Si atoms exhibit a localized nuclear density with weak ADPs (Table 3).

No evidence for new crystallographic site in the apatite structure was found during the refinements for the $La_9SrSi_6O_{26+\delta}$ sample with $\delta = 0.35$ extra oxides, as proposed by Léon-Reina et al. [6]. Structural refinement,
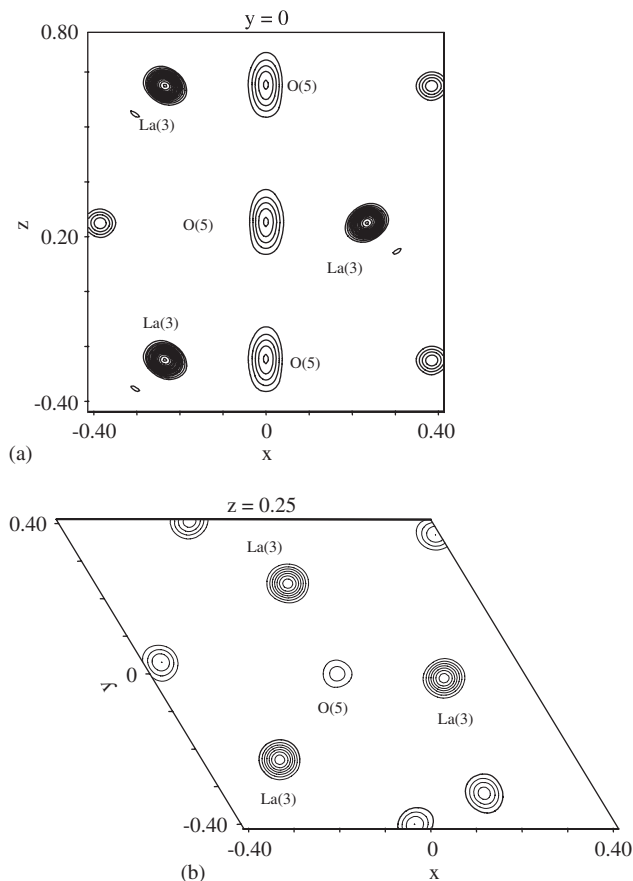
Fig. 4. Fourier maps of the nuclear densities, (a) and (b) along [010] and [001] directions, respectively, calculated $La_9Ba(SiO_4)_6O_{2+\delta}$ compound.
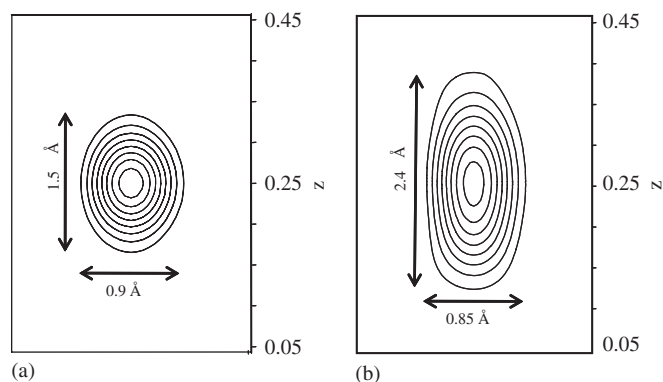


Fig. 5. Calculated Fourier maps of the O(5) nuclear density along the channel, (a) and (b) for $La_{9.33}(SiO_4)_6O_2$ and $La_9Ba(SiO_4)_6O_{2+\delta}$ compounds, respectively.

including an extra site (−0.001, 0.224, 0.580) as described with a very weak occupation (less than 2%) for the $La_{9.55}Si_6O_{26.32}$ compound, is divergent for all the studied samples. The residuum measured at the final refinement (Table 1) is less than 4.2% of the oxygen nuclear density. The extra oxygen does not take part in the coherent neutron diffraction intensity and cannot be considered

localized in the lattice with a long distance order. A part of the $\delta = 0.35$ extra oxygens is probably placed with random distribution in the apatite structure leading to a lattice distortion. This phenomenon could explain the broadening of the peak profile observed on the X-ray diffraction pattern.

The cation-oxygen distances in the studied samples are summarized in Table 4. Inside the [SiO$_4$] tetrahedrons, the Si–O distances undergo very small variation despite the $AE$ doping agent $(1.59(1) < d_{Si-O} < 1.66(1)$ Å) according to the literature [2,11,12]. The bond valence calculation [17] applied to these Si–O bond distances leads to a valence of $+4.0(1)$ for the Si atoms in this tetrahedral environment. This result allows the validation of the bonding scheme for the tetrahedrons. The O(3) nuclear density shows an anisotropic spread along the $a$-axis perpendicular to the channels direction, which is more pronounced for the undoped and the Ca-doped compounds than for the samples with Ba or Sr. This result suggests that the O(3) atoms are vibrating due to electrostatic thrusts (attraction or repulsion) between ions and the distribution of the formal charge (negative in the case of vacancy and positive for $AE$ atoms) of the La(1) and La(2) sites in the crystal [9]. Indeed, the O(5) conduction oxygen is close to the O(3) site of the tetrahedrons $(3.17(2) < d_{O(5)-O(3)} < 3.205(3)$ Å) and leads to probably a slight rotation of the [SiO$_4$] tetrahedron around the Si site in order to obtain some accurate distances at the atomic scale. Concerning the bonding scheme around the conduction oxygen, the O(5) site is close to the La(3) site $(2.2577(1) < d_{O(5)-La(3)} < 2.317$ Å) and this short distance, observed in different structural investigations, is more pronounced for the sample with Ca doping agent (Table 4) than the undoped compound. The nuclear density of the La(3) site exhibits a transverse spread to the O(5) conduction direction in the channels.

In summary, the NPD structural investigations of $La_{9.33}Si_6O_{26}$ and $La_9AE_1Si_6O_{26+\delta}$ ($AE$ = Ba, Sr and Ca)-doped apatites-type lanthanum silicates show the following results. The divalent $AE$ doping agent expands the unit cell of the doped lanthanum silicates in comparison with the $La_{9.33}Si_6O_{26}$ compound. The best description of the structural framework is obtained with the $P6_3$ space group. The 9-coordinated La(1) and La(2) sites contain La, $AE$ and vacancies distributed randomly. The La(3) site is fully occupied by lanthanum atoms. There is no evidence for an extra oxygen site in the apatite structure for the studied compounds. Concerning the conduction atom in the hexagonal channel, no splitting of the nuclear density is observed but instead an anisotropic spread of the nuclear density along the $c$-axis direction. The O(5) conduction oxygen probably induces a slight rotation of the [SiO$_4$] tetrahedron around the Si site in order to maintain interatomic distances. In order to determine the position of the extra oxygen in the material, an investigation by transmission electronic microscopy will be performed. This study will allow us to exhibit the lattice perturbation due to these extra atoms,

Table 4
Selected interatomic distances (Å) in the apatite structure

| | La(1) | | La(2) | | La(3) | | Si | |
|---|---|---|---|---|---|---|---|---|
| Undoped | O(1) | 2.475(17) × 3 | O(1) | 2.524(18) × 3 | O(1) | 2.720(4) | O(1) | 1.610(6) |
| | O(2) | 2.519(17) × 3 | O(2) | 2.586(18) × 3 | O(2) | 2.502(3) | O(2) | 1.627(4) |
| | O(3) | 3.021(9) | O(4) | 2.795(9) | O(3) | 2.578(11) | O(3) | 1.604(10) |
| | | 3.021(11) | | 2.795(13) | | | | |
| | | 3.021(14 | | 2.795(8) | | | | |
| | | | | | O(3) | 2.456(16) | O(4) | 1.655(10) |
| | | | | | O(4) | 2.523(11) | | |
| | | | | | O(4) | 2.474(16) | | |
| | | | | | O(5) | 2.317(2) | | |
| Ba | O(1) | 2.509(8) × 3 | O(1) | 2.518(7) × 2 2.518(8) | O(1) | 2.730(3) | O(1) | 1.637(5) |
| | O(2) | 2.63(1) × 3 | O(2) | 2.51(1) × 3 | O(2) | 2.530(3) | O(2) | 1.622(4) |
| | O(3) | 2.988(2) × 2 2.988(8) | O(4) | 2.808(6) 2.808(5) 2.81(1) | O(3) | 2.545(7) | O(3) | 1.598(7) |
| | | | | | O(3) | 2.543(8) | O(4) | 1.661(8) |
| | | | | | O(4) | 2.670(8) | | |
| | | | | | O(4) | 2.471(9) | | |
| | | | | | O(5) | 2.281(1) | | |
| Sr | O(1) | 2.475(7) × 3 | O(1) | 2.519(7) × 3 | O(1) | 2.741(2) | O(1) | 1.606(4) |
| | O(2) | 2.59(1) × 3 | O(2) | 2.51(1) × 3 | O(2) | 2.522(2) | O(2) | 1.634(3) |
| | O(3) | 2.955(2) × 2 2.955(4) | O(4) | 2.816(4) × 2 2.816(3) | O(3) | 2.576(5) | O(3) | 1.613(6) |
| | | | | | O(3) | 2.487(8) | O(4) | 1.648(6) |
| | | | | | O(4) | 2.609(4) | | |
| | | | | | O(4) | 2.479(7) | | |
| | | | | | O(5) | 2.271(2) | | |
| Ca | O(1) | 2.428(9) × 3 | O(1) | 2.507(9) × 3 | O(1) | 2.770(3) | O(1) | 1.616(4) |
| | O(2) | 2.59(1) × 3 | O(2) | 2.44(1) × 3 | O(2) | 2.539(2) | O(2) | 1.629(3) |
| | O(3) | 2.968(2) × 2 2.968(7) | O(3) | 2.779(5) × 2 2.78(1) | O(3) | 2.583(9) | O(3) | 1.644(9) |
| | | | | | O(3) | 2.44(1) | O(4) | 1.59(1) |
| | | | | | O(4) | 2.648(9) | | |
| | | | | | O(4) | 2.49(1) | | |
| | | | | | O(5) | 2.258(1) | | |

and thus lead to essential information regarding the conduction mechanism.

## References

[1] S. Beaudet Savignat, A. Lima, A. Brisse, C. Barthet, J. Am. Ceram. Soc. (2006), to be published.
[2] L. Leon-Reina, E.R. Losolla, M. Marthinez-Lara, S. Bruque, M.A.G. Aranda, J. Mater. Chem. 14 (2004) 1142.
[3] S. Nakayama, M. Sakamoto, J. Mater. Sci. Lett. 20 (2001) 1627.
[4] A. Vincent, S. Beaudet-Savignat, F. Gervais, J. Eur. Ceram. Soc. (2005), to be published.
[5] S. Nakayama, T. Kageyama, H. Aono, Y. Sadaoka, J. Mater. Chem. 5 (1995) 1801.
[6] L. Leon-Reina, M.C. Martin-Sedeno, E.R. Losilla, A. Cabeza, M. Martinez-Lara, S. Brusque, F.M.B. Marques, D.V. Sheptyakov, M.A.G. Aranda, Chem. Mater. 15 (2003) 2099.
[7] Y. Masubushi, M. Higuchi, T. Takeda, S. Kikkawa, Solid State Ion. 177 (2006) 263.
[8] H. Okudera, A. Yoshiasa, Y. Masubuchi, M. Higuchi, S. Kikkawa, J. Solid State Chem. 177 (2004) 4451.
[9] H. Okudera, Y. Masubuchi, S. Kikkawa, A. Yoshiasa, Solid. State Ion. 176 (2005) 1473.
[10] J.E.H. Sansom, D. Richings, P.R. Slater, Solid. State Ion. 139 (2001) 205.
[11] J.E.H. Sansom, J.R. Tolchard, P.R. Slater, M.S. Islam, Solid. State Ion. 167 (2004) 17.
[12] J.R. Tolchard, M.S. Islam, P.R. Slater, J. Mater. Chem. 13 (2003) 1956.
[13] H. Arikawa, M. Nishiguchi, T. Ishibara, Y. Takita, Presented at 12th International Conference of Solid State Ionics, 1999.
[14] H. Yoshioka, J. Alloys Compds. (2005), to be published.
[15] E.J. Abram, D.C. Sinclair, A.R. West, J. Mater. Chem. 11 (2001) 1978.
[16] V. Petricek, M. Dusek, Institute of Physics, Praha, Czech Republic.
[17] N.E. Brese, M.O. Keeffe, Acta Cryst. B (1991) 192.
[18] K.N. Trueblood, H.B. Burgi, H. Burzlaff, J.D. Dunitz, C.M. Gramaccioli, H.H. Schulz, U. Shmueli, S.C. Abrahams, Acta Cryst. A (1996) 770.